Lifetime Modeling for JEDEC Drop Tests

Frank Krämer[1], Sven Rzepka[2], Jens Lienig[3]

[1] Fraunhofer Center for Silicon Photovoltaics

Walter-Huelse-Strasse 1, 06120 Halle (Saale), Germany

frank.kraemer@csp.fraunhofer.de, phone: +49 345 5589 425

[2] Qimonda Dresden GmbH & Co OHG, Dresden, Germany

[3] Dresden University of Technology, Institute of Electromechanical and Electronic Design, Germany

Abstract

Since lead was banned from the solder joints, mechanical tests of microelectronic components and modules have gained much importance not just in mobile electronics but quite in general. The standardized JEDEC drop test is commonly used. It delivers repeatable results for a wide range of loads in the components mounted on the well specified test PCB. As yet the JEDEC drop test is time consuming and thus expensive, the goal of this study has been to develop a lifetime model for virtual assessments of the drop test performance by means of FEM simulation. The development started with assuring that the dynamic PCB deformation is captured precisely. Hereby, the constraint conditions were found to be most influential for minimizing the differences between the acceleration curves measured and the FEM simulation results (LS-Dyna). Subsequently, a number of known result criteria were evaluated by means of their capability to estimate the sequence of component failures within the experiments. It turned out that none of the criteria was able to predict the failure sequence accurately. Therefore, a new criterion was composed. Combining plastic strain rate and resulting force integral, the experimental failure distribution was matched perfectly for all three package types investigated. The lifetime model based on the combined criterion was able to forecast the experimental number of cycles to failure with less than ±25% inaccuracy.

Introduction

Since the ban of lead from the solder materials, dynamic mechanical integrity has become of high concern to all microelectronics applications. The new solder alloys are stiffer. They induce higher stress into the layers of intermetallic compounds (IMC) at the solder / pad interfaces. Hence, module level drop tests are typically conducted to proof the mechanical reliability to suffice. As with all such experiments and their preparation, these practical test are time consuming and expensive. Hence, the attempt has been made in the past two years to develop a lifetime model, based on which drop tests can be conducted virtually by means of explicit FEM simulation.

The development of a trustworthy lifetime model requires a reliable experimental setup generating repeatable and well defined results. The JEDEC drop test [1] offers such a setting. Mounting 15 components on a test PCB being specified in very detail, a quite comprehensive set of data can be collected within every test. Depending on the position on the board, each component is exposed to its individual load level with a wide range covered simultaneously by the test. Consequently, the sequence, at which the components fail during repetitive drops, can be used to evaluate the different simulation result criteria that are known for being used in assessments of dynamic mechanical events. The criterion suitable for developing a lifetime estimation model must be able to estimate the experimental failure sequence well. Otherwise, the targeted accuracy of ±50% can not be reached for predictions of the number of cycles to failure.

The following sections detail the experimental setup, the simulation models, the assessment criteria evaluated, as well as the development of the final assessment criterion and the lifetime model. Finally, the validity of the methodology is varified by comparing the lifetime predictions of three different types of packages to experimental data.

Experimental setup

The JEDEC Standard JESD22-B111 [1] prescribes the specimens, the load conditions, and the general setup of a commonly used mechanical drop test. Because of its high reproducibility, this method is applied to select the solder ball compositions and the pad finishes for adequate performance during drop tests. Hence, it can also be used for developing a virtual drop test method.

A commercial drop test setup has been used during the study at Qimonda. The drop tower is shown in fig. 1. The sledge is mounted between two guiding rods, which are fixed to a solid base plate. During the test, the sledge is dropped onto the base plate. Here, different felt layers can be placed. They control the specific deceleration profile of the sledge when dropping, i.e., the drop pulse to comply with conditions of the standard [1]. On its top side, the sledge can be equipped with different mounting plates accommodating various PCB sizes and providing for different boundary conditions including all fixture specifications also defined by the JEDEC standard.

The measurement equipment attached to the drop tower allows in-situ recording of the acceleration at the
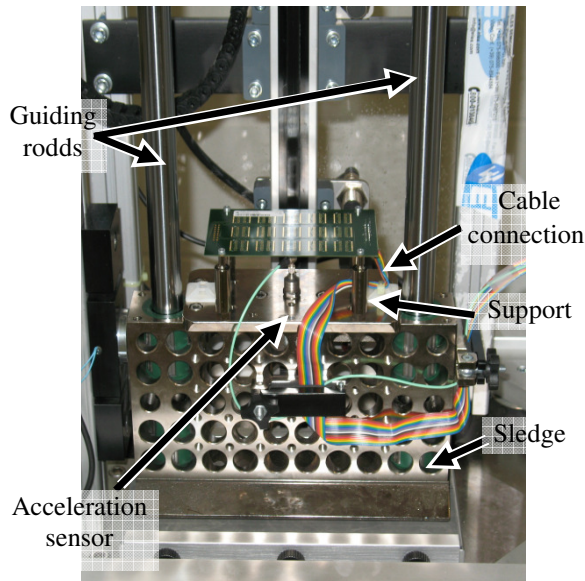
—1—

Figure 1: Drop Test Tower with base plate, sledge and guiding rods. A JEDEC Drop Test board is mounted on the sledge and connected to the in situ resistance measurement

drop table and at one point at the sample. In addition, it provides for monitoring the electrical resistance of the daisy chain at the test sample continuously as well as by means of an event detector. This way, the electrical open causing a resistance of 1kΩ or more is captured without delay.

Three different packages have been used in this study with daisy chains covering almost all of its interconnections. The geometrical data of the components is listed in table 1 together with the I/O configurations. The packages cover the field of quasi quadratic arrangements of the SnAg1Cu0.5 solder balls to strongly rectangular ones. According to the typical high volume situation, ENiG pad finish was used on component side while the PCB pads came with CuOSP.

Label	VFBGA-90	VFBGA-60	TFBGA-60
Height [mm]	0.8	0.8	1.2
Package area [mm]	12.5 x 9.5	10.0 x 9.5	10.5 x 8.0
Number of Balls	90	60	60
Ball-out size [mm]	11.2 x 6.4	7.2 x 6.4	8.0 x 6.4
Ball arrangement	15 x 6, full rows	10 x 6, full rows	11 x 6, partly populated

Table 1: Geometrical properties of the test samples

The majority of the tests were done using the JEDEC condition B. The sinusoidal acceleration impulse has a peak of 1500 G and a duration of 0.5 ms measured at the top surface of the sledge (fig. 1). This test condition lead to failure rates between 10 and a few 100 drops across all tested components.

The acceleration profile at the sledge defines the pulse applied to the test PCB. Dependent on the way the PCB is mounted onto the sledge, specific eigenmodes and eigenfrequencies are excited in this specimen. The resultant deformation of the PCB finally determines the specific load at each component site and thus the sequence of the components to fail as well as the particular joint eventually causing this failure.

Within this study, two kinds of boundary conditions have been considered. They are shown in fig. 2. Condition a) stands for the 4-screw fixture as it is proposed by the JEDEC standard. Fixing the corners only, the amplitude of PCB deflection is large than in case b), in which the long edges of the PCB are constraint by additional screws in their center. The difference in PCB clamping has a big influence on the resulting vibration frequencies. While the first natural frequency is about 180 Hz in case of the 4-screws configuration, it is increased to about 390 Hz in case of the 6-screws fixture. Thus, less than half of the speed is generated in the 4-screws settings as compared to the 6-screws configuration resulting in smaller dynamic loads on the components and their interconnections. Beside the vibration frequency, the PCB deformation and, thus, the stress distribution across the board is changed significantly leading to different specific loads at all component positions. The effect of these differences in dynamic PCB deformation on the experimental results will be discussed in the next section.

Experimental results and discussion

At the pad/solder interfaces, intermetallic compounds like Cu_6Sn_5 and $(Ni, Cu)_3Sn_4$ are formed during soldering. They are quite brittle. In addition, lead-free solders are stiffer than lead containing materials. Therefore, more stress is transferred to the IMC at the drop events and the risk of brittle cracks is increased. Consequently, brittle IMC cracks were expected to be the dominating failure mode as also observed before [2-6].

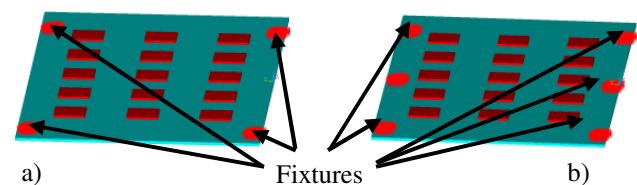The experiments started with the 4-screws fixture.

Figure 2: PCB fixture conditions: a) 4-screws fixture according to JEDEC standard; b) 6-screws fixture with additional fixture at the PCB center
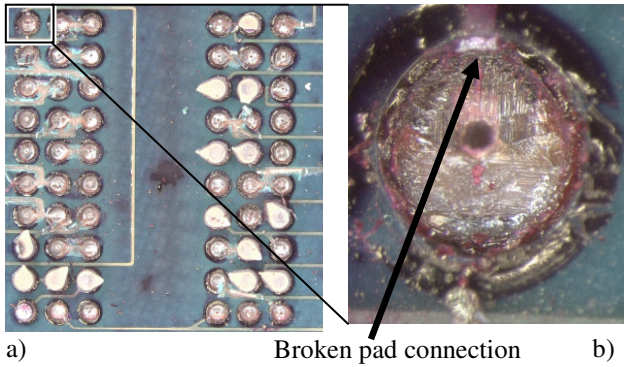
a)   Broken pad connection   b)

Figure 3: Failure analysis with the dye and pry method. a) Total component ball-out; b) Ball-out section with electrical fail, caused by a broken copper trace

VFBGA-90 packages (tab. 1) were attached to JEDEC test boards having a similar laminate stack as the actual memory modules, i.e., 8 layer core material was used. Applying the JEDEC drop condition B (1500 G, 0.5 ms), the subsequent failure analysis surprisingly showed no IMC failures at all. Instead, the dye and pry tests revealed PCB pad lifts as the dominant failure triggering mode (fig. 3). Lifting the pads, the copper trace connected to them broke and caused the interruption of the daisy chain.

The tests with the 6-screws fixture showed the same failure mode. The increase in the 1st natural frequency and the change in deformation pattern and speed did not alter it. Only the N_{63}, the characteristic number of cycles to failure of the Weibull distribution, reduced significantly. The most critical component characteristically failed after 126 drops in case of the 4-screws fixture while it endured 43 drops only when the 6-screws fixture was used. In all cases, however, the dye and pry tests clearly showed the electrical fails being caused by broken copper traces at lifted PCB pads. IMC cracks were found rarely and only after the electrical failure had already occurred at other interconnections.
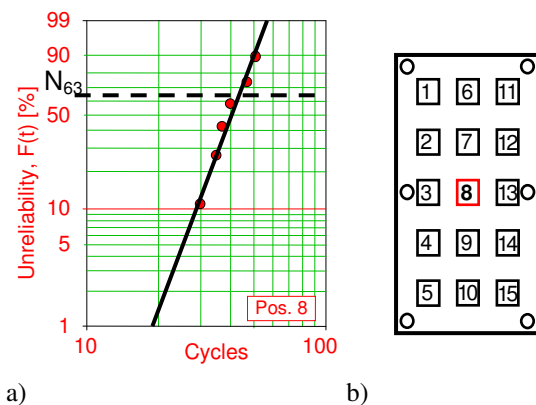

Figure 4: a) Weibull plot of experimental cycles to failure, 6-screws test, package type VFBGA-90, component position #8; b) Numbering of the component positions

Finally, drop tests conducted on several memory module products also brought up this mode as dominating root cause of the failure. Therefore, the focus of the lifetime model under development was shifted to capture the PCB pad lifts.

As mentioned before, the lifetime model aimed to predict the sequence of component failures across the JEDEC board. Therefore, the experimental tests had to be extended up to the point when enough failure data is collected at each of the 15 component positions of the test board to allow fitting it by Weibull distributions.

As an example, figure 4 shows the Weibull fit of a component at position #8 with the minimum sample size allowed in this test. The first failure occurred at 30 drops; the last failure occurred after 51 drops. This is a typical range also seen in tests of other groups [6, 7].

Table 2 compiles the N_{63} values of the Weibull distribution of all investigated packages (see table 1) at the five most critical component positions and lists the sequence of failures. The failures concentrate in the middle row of the test PCB as the 6-screws fixture is used. In this configuration, the PCB is mainly deformed along its width while the long edges remain almost straight. In the case of 4-screws fixture, the deformation takes place along both, the long and the short side of the PCB with the maximum deflection occurring in the center. This induces more stress at the diagonal component positions 2, 4, 12, and 14 (fig. 4b) at the outer rows of the test board, causing these components to fail quite early [8]. In this study, the focus was set on the 6-screws configuration. The 4-screw tests are reserved for future work.

FEM Models for JEDEC Drop Test Simulations

In this study, LS-Dyna™ was used to simulate the highly dynamic drop test events. Figure 5 shows the geometric model. The JEDEC test board is modeled fully, i.e., without involving any symmetry or repetitive conditions, in order to account for all important eigenmodes. The PCB is represented by shell elements. They are ca-

Table 2: Characteristic number of cycles to failure, N_{63}, and failure sequence of the most critical component positions for all 3 package types tested in 6-screws configuration

Package type	VFBGA 60	VFBGA 90	TFBGA 60
Comp 06	-	88.7 (4)	-
Comp 07	290.6 (3)	93.9 (5)	161.2 (3)
Comp 08	89.7 (1)	43.1 (1)	67.6 (1)
Comp 09	141.4 (2)	58.4 (2)	112.8 (2)
Comp 10	-	69.5 (3)	-

10th. Int. Conf. on Thermal, Mechanical and Multiphysics Simulation and Experiments in Micro-Electronics and Micro-Systems, EuroSimE 2009
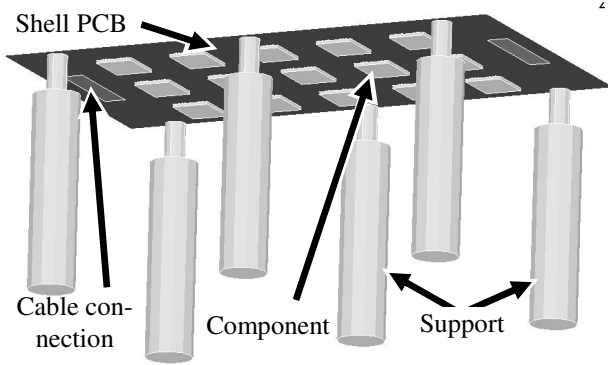
Figure 5: FEM net of the JEDEC Drop test model with its specific features

pable of modeling all bending and tensile loads, which are acting on the PCB during the drop event. The shell elements also provide for applying the LS-Dyna material model #117 [9] (*MAT COMPOSITE MATRIX) that allows entering the properties of the PCB in matrix form after computing them according to the laminate theory [10,11]. With this material model it is possible to realistically account for the differences in tensile and bending stiffness of the actual PCB.

At both short edges of the board, arrays of plated through hole vias are located, which may be used for the cables required by the in-situ resistance measurement. In this study, cables are attached to just one of the two areas because the boards were populated with components on one side only. As seen in figure 6, the cables have a significant effect on the deformation of the PCB. The vibration frequency is not changed but a strong damping effect occurs next to the cable connection. The acceleration amplitude declines muc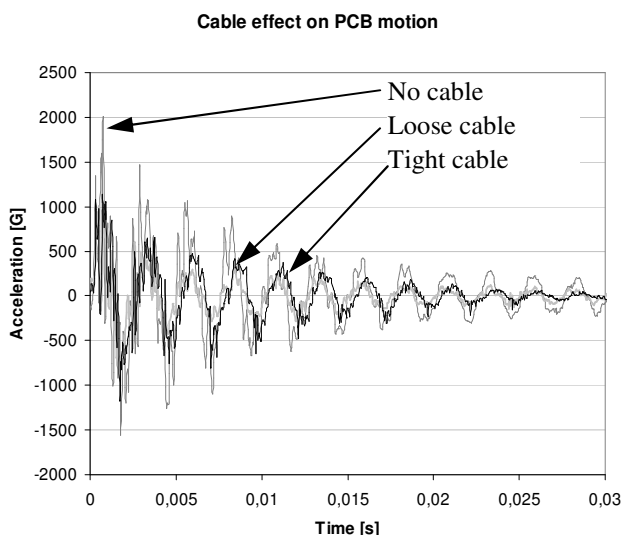h faster than in case of the free via array (with no cables connected). Therefore, additional damping needs to be introduced in to the simulation model for the sake of matching the experimental PCB behavior. In addition, figure 6 also indicates the tightness of the cable to modify the deformation magnitude. Its effect on the acceleration magnitude is only small. Still, it strongly influences the number of cycles to failure at several component positions. Hence, the setting of this specific damping value shall be adjusted carefully.

Besides geometry and material of the test board, its load and boundary conditions need to be modeled precisely. The acceleration reading that was recorded on the sledge during the experiments is directly taken as load input. It is applied to the constraints. In the simplest case, they are placed directly on the PCB at the positions of the fixture holes. However, the computed results would then differ much from the ones measured at the PCB. Figure 7 shows the vibration frequency and the peak acceleration values to be higher than they are in reality when the simple simulation is used. Adjusting the material model is not the right way of counter-acting as the PCB stiffness would need to be reduced below 2 GPa, i.e., to less than 10% of its actual magnitude.

So, the support legs between the sledge and the PCB have to be included in the model to effectively soften the PCB response simulated as seen in fig. 5. These steel cylinders having a diameter of 12 mm and a height of 60 mm are modeled by solid elements and attached to the PCB shells by contacts. Including the legs in the model, the simulation result can follow the measured acceleration curve very closely. At the central position (component #8), which is shown in figure 7, the remaining root-mean-square difference between measured and simulated acceleration curves declined by 72% as compared to the case of the simple model. Obviously, the support legs are not perfectly rigid but contribute to the deformation during the drop event. They lower the overall stiffness of the system.

Figure 6: The effect of the cable connected to the test board on the local acceleration
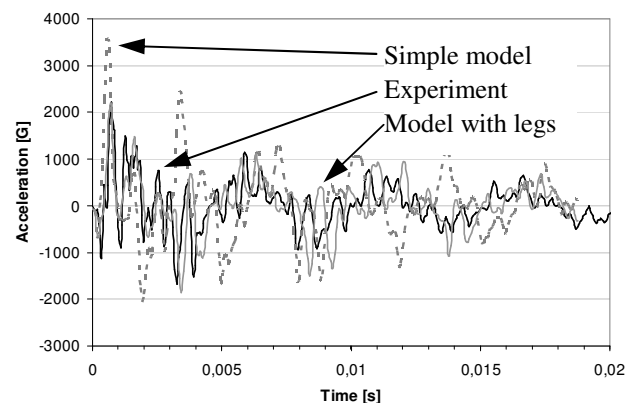

Figure 7: Effect of the boundary conditions on the accuracy of the simulated acceleration results

It was found adequate to model the component in a rather simple way consisting of a hexahedral body and the solder joints as seen in figure 8. Effective elastic properties similar to those of mold compound have been assigned to the component body. The solder balls are modeled as cubes meshed by eight identical elements. Only the most critical joints at the outer rows are modeled as barrels closely replicating the actual dimensions at both pads as well as at the equator of the joint. These joints are meshed by 24 elements, which still lead to a rather coarse mesh yet being sufficient for the attempted lifetime modeling. The solder balls use the plastic material model with kinematic hardening. As shown in figure 8, the solder balls are directly attached to the component. On the other end, offset contacts are applied to connect the joints to the PCB.

Based on the set of models developed in this study, the experimental deformation profile of the test PCB is matched very closely by the transient dynamic simulation for all component positions at the JEDEC test board. This is the essential basis for computing the correct stress magnitudes and distribution in and at each solder ball.

Introduction and discussion of result criteria

Lifetime modeling requires an adequate failure criterion, which can quantify the effects triggering the failure mode seen in the experiments. This section reviews the options available for virtual lifetime estimation of JEDEC drop tests. They can be grouped into two classes, continuum mechanics and fracture mechanics criteria, respectively.

The bending moment induced into the PCB during the drop impact would be a first continuum mechanics criterion [12-14]. It has been proposed based on the observation that the failure of the solder balls is caused by the stresses resulting from the differences in bending between PCB and component. However, focusing on the PCB side only, this criterion is unable to cover any changes in package configuration and solder alloy. Therefore, it can not serve as general lifetime criterion and, hence, it is not considered further by this study.
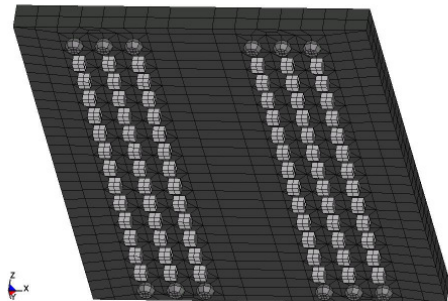

Figure 8: Single component of the global JEDEC Drop Test model

Other result criteria directly address the load situation within the individual solder balls. This way, they do account for the details of package configuration and solder alloy. The plastic strain, ε_p, accumulated in the solder ball during a drop event is one of these criteria [15-18]. A plastic deformation occurs only when the stress in the solder exceeds the yield point, i.e., when the joint is deformed irreversibly. Since the eventual failure really is caused by inelastic effects, the criterion 'plastic strain' appears as a suitable lifetime criterion. On the other hand, the accumulated plastic strain is an integral criterion that covers the full drop event without distinguishing between different load pulses. Hence, it may be able to predict the failure but without capturing the effect of the deformation speed, i.e., it will not be able to recognize whether the failure was due to ductile fatigue (in the solder) or brittle cracks (e.g., at the pad PCB interface) [19].

The plastic strain rate, $\dot{\varepsilon}_{pl}$, [18-21] overcomes the limitations of the plastic strain. Again, it is larger than zero only if the stress is above the yield level, i.e., when the essential condition for failure initiation is fulfilled. In addition, the strain rate also accounts for the speed of failure creation and propagation. This way, it has already been applied to failure mode characterizations successfully [19]. On the other hand, this criterion is quite sensitive to inaccuracies. It is deduced by differentiating the primary solution of the FEM equation twice, once with respect to space obtaining the strain and once more with respect to time for deducing the rate. Hence, the computed magnitude of the plastic strain rate does not only depend on real effects like the position of the solder ball on the PCB but is affected by modeling details like the mesh size as well. In terms of the time domain, not only the real deformation speed but also the simulation time steps may alter the magnitude. Consequently, the strain rate criterion allows reliable predictions only when the transient PCB deformation during the drop event is modeled very precisely.

Alternatively to the strain, the resulting force, F, is also proposed as criterion [22]. Computed at the interface between PCB and solder ball, this criterion evaluates the force vector acting on the contact area. It includes tensile and shear contributions. Since the diameter of the PCB pads is the same in all the investigated packages, this criterion also allows direct result comparisons. Similar to the plastic strain rate, the magnitude of the resulting force may be affected by bad time stepping. Integration would overcome this problem. The time interval can be determined by a second result parameter such as the occurrence of a non-zero plastic deformation in the solder ball. This way, the magnitude of the integrated resulting force, $\int F \, dt$, is not dominated by the elastic part of the load history. With the solder entering the plastic range, the slope of

stress vs. deformation also is lowered for the copper pads because joints and pads constitute a chain configuration with the solder ball being the weakest link. Hence, the criterion ∫F dt is able to cover both, ball and pad failures.

The first principal stress, σ_1, is another criterion applied to drop test assessments [14, 16, 23-25]. Because of the loading conditions in a drop test, the peak value of σ_1 coincides with the peel stress. After determining the thresholds for the interface cracks to occur, the first principal stress may be chosen as criterion for quantifying the risk of pad peeling. Of course, these thresholds are sensitive to many specifics at the interfaces involved. Hence, quite comprehensive experimental studies are needed before this criterion could be used as general lifetime criterion.

The van-Mises-stress, σ_{EQV}, has also been proposed as lifetime criterion [26]. It basically stands for the vector sum of the differences between the principal stress components. When clearly being dominated by the tensile stress, this criterion would behave quite similarly to the first principal stress with no extra benefit. If the other two components also show substantial magnitudes, the inability of σ_{EQV} to distinguish between tensile and compressive contributions really turns out as a disadvantage. Therefore, the van-Mises-stress criterion is not seen suitable and, thus, disregarded in this study.

The last group of continuum mechanics criteria proposed for lifetime estimation concern the mechanical energy, W, accumulated in the solder ball during one load cycle [22, 27, 28]. The energy is an accumulating criterion, which is dominated by inelastic deformations. Similar to the force integral mentioned before, it might also be suited to characterize the failure in the copper traces due to pad lift. Being the product of stress and strain, mechanical energies are typical element simulation results. Still, care must be taken on what stress and strain parameters are chosen exactly. In case of the drop test, the energy criterion should be based on the plastic strain in the solder.

The stress intensity factor is the most popular representative of the group of fracture mechanics criteria [2]. It allows computing the crack growth during each single shock pulse based on the stresses occurring at the crack tip. The J integral concept would widen the applicability to nonlinear stress fields. Due to the highly singular nature of the stress situation, applying these criteria would require very fine meshes at the crack tip. In many cases, sub-modeling techniques allow covering the large range of dimensions between crack tip and full module. In case of the JEDEC drop test, however, a minimum of 120 different crack positions would have to be considered simultaneously (15 components, 4 most critical solder joints, at least 2 - more likely 4 - crack sites per joint). At present time, no concept is known that would allow handling this situation in a transient dynamic simulation. The resources

required would be excessively large. So, the stress intensity factor and J integral seem to be not applicable at the moment.

Energy release rate and Griffith's energy relation provide alternative fracture mechanics concepts. Both theories are valid for brittle cracks with negligible plastic deformations around the crack tip. They might be applied to the crack of copper trace but would again lead to much higher computational efforts then required by the continuum mechanics criteria, which have also given hope for being suitable. Therefore, this study focuses on the continuum mechanics criteria.

Result criteria application on the experimental failure arrangement

The assessment of the failure criteria is done by comparing the experimental order of failure occurrence among the 15 components of the JEDEC drop test board to the sequence of failure occurrence predicted by simulation. Since all the criteria quantify a load, the lifetime depends inversely on them. Specifically, the inverse power law is seen applicable. Therefore, the highest magnitude shows the component, which – according to the respective criterion – is supposed to fail first. The first round of assessing the criteria is based on the experimental results of the VFBGA-90 components (table 2). The outcome of the evaluation is compiled in table 3, which also includes the component positions #3 and #13 (fig. 4).

An error parameter was introduced for the objective assessment of the criteria. It is deduced from the absolute difference in the order of failure predicted by the simulation, OF_{SIM}, and that found in the experiment, OF_{EXP}. According to equation (1)

$$\text{ERR} = \sum_i \psi \left| OF_{SIM} - OF_{EXP} \right|, i = 3, 6, \ldots 10, 13 \ (1),$$

the total error, ERR, is the sum of the errors at each component i multiplied by a weight factor ψ reflecting the highest importance of accurate predictions at the most critical components #8 … #10. For each criterion separately, the total error, ERR, is listed in the bottom row of table 3.

The value of ERR is quite different among the criteria. The first principal stress, σ_1, which was proposed by most often, and the solder ball energy, W, which is directly available in the FEM tools, lead to the highest ERR parameters, i.e., they predicted the sequence of failure occurrence with lowest accuracy. In particular, both criteria have not been able to identify the most critical component position right. Moreover, the magnitude of the principal stress is almost the same at all component positions. It varies by 5% only while the experimental number of cycles to failure varies by a factor of more than five. Hence, these two criteria are not suitable for lifetime models of drop tests.

On the other hand, quite high prediction accuracy was achieved when applying the criterion of plastic strain, ε_{pl}, and – even more – that of plastic strain rate, $\dot{\varepsilon}_{pl}$. Both criteria clearly point to position #8 as the most critical component. In addition, the plastic strain rate correctly predicts that almost all components of the center row are more critical than the components #3 and #13 placed at the outer rows that failed only very late in the experiment.

When applying the criteria of resulting force, F, and resulting force integral, ∫F dt, the experimental failure sequence is also matched rather well. Only component #13 is wrongly highlighted as the most critical one. When disregarding this artifact, even the distribution of the criteria magnitudes nicely follows that of the inverse experimental number of cycles to failure. Obviously, the artifact consists of a sharp force peak that impairs the prediction accuracy at position #13 – affecting the force criterion more then the force integral.

Assessing all criteria, the plastic strain rate ranks first. Still, it shows differences in the order of failure to the experiment in four of the seven component positions included in table 3. When applying the integrated force criterion, the direction of the differences in the order of failure is almost inversed to those found with the plastic

strain rate (except for position #13). The combination of both criteria yields the plastic strain energy density, SEND, if the force is transformed into a stress value according to equation (2)

$$\text{SEND} = \int \dot{\varepsilon}_{pl} \cdot \frac{F}{A_{Pad}} \, dt \qquad (2)$$

with A_{Pad} being the pad area, on which the force is acting. This new criterion is able to predict the experimental failure arrangement most precisely. All components of the center row (#6 … #10) are realistically found more critical than the components #3 and #13. There is only one mixing in the failure sequence left – positions #6 and #7. Considering the respective magnitudes of cycles to failure and of the criterion SEND, the differences between these two positions are rather small indeed. Hence, this simulated misstep is tolerable.

The result of a quantitative accuracy check is shown in figure 9. Besides the close match of the failure sequence, the SEND values also support the inverse proportional lifetime model. The correlation coefficient, R^2, is larger than 90%, which proves this criterion's ability to predict the measured cycles to failure almost perfectly. The remaining inaccuracy is as small as ±20%. Hence, the initial target of maximum ±50% inaccuracy was clearly met.

Comp. Number: Experimental Cycles to Failure, N_{63} (OF$_{EXP}$)	Error Weight Factor, ψ	Plastic strain, ε_{pl} [%] (OF$_{SIM}$)	Plastic strain-rate, $\dot{\varepsilon}_{pl}$ [s^{-1}] (OF$_{SIM}$)	Resulting force, F [N] (OF$_{SIM}$)	Integrated resulting force, ∫Fdt [N·ms] (OF$_{SIM}$)	Principal stress 1, σ_1 [MPa] (OF$_{SIM}$)	Solder ball energy, W [mJ] (OF$_{SIM}$)	**Strain energy density, SEND [mJ/mm³] (OF$_{SIM}$)**
Comp #3: >200 (7)	1	1.5 (7)	51.9 (7)	5.2 (7)	16.9 (7)	86.1 (**2**)	0.191 (**2**)	**8.5 (7)**
Comp #6: 89 (4)	1	4.4 (6)	79.3 (**3**)	7.6 (3)	27.4 (6)	85.1 (4)	0.160 (4)	**21.7 (5)**
Comp #7: 94 (5)	1	7.8 (5)	68.7 (6)	7.5 (5)	31.7 (5)	83.7 (6)	0.106 (7)	**21.8 (4)**
Comp #8: 43 (1)	**3**	14.6 (**1**)	119.5 (**1**)	7.9 (**2**)	38.0 (**2**)	82.4 (7)	0.188 (**3**)	**45.2 (1)**
Comp #9: 58 (**2**)	**2**	9.1 (**3**)	93.9 (**2**)	7.6 (**3**)	34.5 (**3**)	85.1 (4)	0.126 (6)	**32.4 (2)**
Comp #10: 70 (**3**)	**2**	8.5 (4)	73.4 (4)	7.5 (5)	33.3 (4)	85.6 (**3**)	0.131 (5)	**23.8 (3)**
Comp #13: 105 (6)	1	10.1 (**2**)	70.2 (5)	8.6 (**1**)	39.7 (**1**)	86.6 (**1**)	0.207 (**1**)	**21.0 (6)**
Error, ERR Comment		10	5 2nd Best	15	15	35 Worst	30 2nd Worst	**2 Best**

Table 3: Order of failures, OF, determined in the experiments and predicted based on several failure criteria
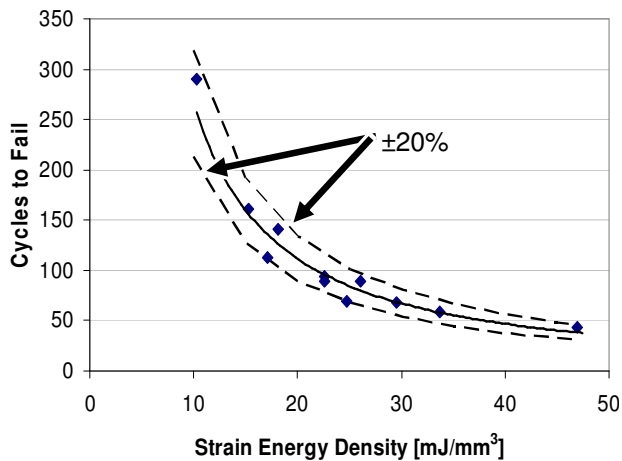
Figure 9: Correlation between strain energy density and real cycles to failure (VFBGA-90 component)

A Lifetime Model for the JEDEC Drop Test

In order to validate the novel criterion SEND, it has been applied to further components, whose experimental cycles to failures are also listed in table 2. Due to full parameterization, the geometric model only requires the corresponding dimension and ball-out parameters to be changed to the values listed in table 1. No changes are needed with respect to the contact elements joining PCB and component as well as in the boundary conditions since the experimental setup remains the same. Therefore, the new simulation results can directly be compared to those of the VFBGA-90 component.

Based on the available experimental and simulation result, a lifetime model was set-up in form of a simple inverse power law as given by Equ. (3):

$$N_{63} = C_1 / (\text{SEND})^{C_2} \qquad (3)$$

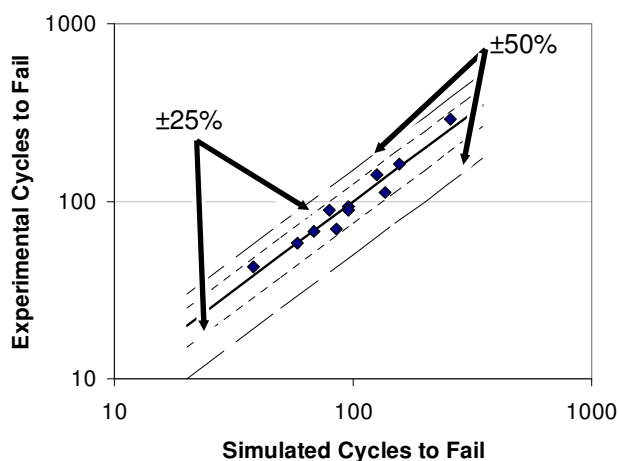Pre-factor, C_1, and exponent, C_2, are determined based on

Figure 10: Comparison of simulated and experimental cycles to fail

the simulated SEND values and the measured characteristic failures, N_{63}, of the components VFBGA-60, VFBGA-90, and TFBGA-60. The comparison between the simulated and the experimental lifetime is shown in figure 10. A close match can be seen between prediction and reality. Even the maximum difference does not exceed ±25%, which is in the same range of the most advanced lifetime models for temperature cycling. Of course, this also meets the original target of ±50%. When assessing each component position in detail, all simulation predictions match the experimental results well within the experimental range of scatter. This means, the simulation results are as close to the characteristic number of cycles to failure as the experiment. Therefore, the criterion SEND is well suited for being used in lifetime modeling. It even provides a level of prediction accuracy that suffices for virtual prototyping studies to be conducted.

Conclusion

The results of a two years industrial methodology effort on a virtual lifetime model development for the JEDEC drop test have been reported. Detailed experimental studies were done with three different types of memory components as reference tests. Based on the development of the experimental methodology, these components were subjected to a JEDEC drop test. The only modification introduced concerned the PCB fixture at six points instead of four as seen in figure 2b. This resulted in more realistic number of cycles to failure as compared to field conditions while the dominating failure mode was still PCB pad lift. The PCB stack-up was according to the one proposed in the standard [1]. Typical load was the JEDEC condition B, i.e., a peak acceleration of 1500 G and pulse duration of 0.5 ms.

Before the assessment of possible result criteria, a new simulation methodology was introduced. It centered on detailed investigations of the PCB motion during the drop event as this provides the basis for all the lifetime predictions. Besides applying the laminate theory to really model the actual PCB stack well, the boundary conditions and the effects of the cable connection have been studied in detail in order to make sure, the transient PCB deformation is captured most closely.

Afterwards, typical result criteria were assessed by comparing the experimental and the predicted failure ranks. It turned out that none of the criteria proposed in literature were able to predict the experimental failure rank without numerous flaws. Therefore, a new failure criterion was developed combining the plastic strain rate and the force integral to yield strain energy density, SEND. This criterion was able to predict the experimental failure ranks of all the three packages correctly. Furthermore, a lifetime model was established, which has been able to predict the experimental number of cycles to failure with an inaccuracy range as low as ±25%. This

10th. Int. Conf. on Thermal, Mechanical and Multiphysics Simulation and Experiments in Micro-Electronics and Micro-Systems, EuroSimE 2009

accuracy does not exceed the experimental scatter and is beyond the original target.

Acknowledgments

References

1. Jedec Standard JESD22-B111, Board Level Drop Test Method of Components for Handheld Electronic Products

2. Yu/ Kikuchi/ Ikeda: Dynamic Behavior of Electronics Package and Impact Reliability of BGA Solder Joints. Inter Society Conference on Thermal Phenomena 2002.

3. Desmond/ Chong/ Che: Drop Impact Reliability Testing for Lead-free and Lead-based Soldered IC Packages. Microelectronics Reliability 46 (2006), p1160-1171.

4. Tee/ Ng/ Lim: Impact Life Prediction Modeling of TFBGA Packages under Board-Level Drop Test. Microelectronics Reliability 44 (2004), p87-94.

5. Syed/ Kim/ Cha: Effect of Pb free Alloy Composition on Drop/Impact Reliability of 0.4, 0.5 & 0.8mm Pitch Chip Scale Packages with NiAu Pad Finish. Electronic Components and Technology Conference (ECTC) 2007.

6. Luan/ Goh/ Baraton: A Novel Methodology for Virtual Qualification of IC Packages under Board Level Drop Impact. ECTC 2008.

7. Wang/ Hung/ Jiang: High Drop Performance Interconnection: Polymer Cored Solder Ball. ECTC 2008.

8. Lai/ Yang/ Yeh: Experimental Studies of Board-Level Reliability of Chip-scale Packages Subjected to JEDEC Drop Test Condition. Microelectronics Reliability 46 (2006), p645-650.

9. Livermore Software Technology Corporation: LS-DYNA Keyword User's Manual; May 2007, Version 971. www.lstc.com

10. Tsai/ Hahn: Introduction to Composite Material, 1980. Technomic Publishing Company, Inc., ISBN No. 0-87762-288-4

11. Krämer/ Rzepka/ Grassmé: A Multilayer PCB Material Modeling Approach Based on Laminate Theory. EuroSimE 2008.

12. Wong/ Mai: New Insights into Board Level Drop Impact. Microelectronics Reliability 46 (2006), p930-938.

13. Wong/ Mai/ Seah: Board-Level Drop Impact – Fundamental and Parametric Analysis. Journal of Electronic Packaging, Vol. 127, Dec2005, p105-108.

14. Che/ Pang/ Zhu: Comprehensive Modeling of Stress-Strain Behavior for Lead-Free Solder Joints under Board-Level Drop Impact Loading Condition. ECTC 2007.

15. Lall: Computational Methods and High Speed Imaging Methodologies for Transient Shock Reliability of Electronics. EuroSimE 2007.

16. Lai/ Yeh/ Wang: Investigations of Board-Level Drop Reliability of Wafer-Level Chip-Scale Packages. Journal of Electronic Packaging, Vol. 129, Mar2007.

17. Syed/ Lin/ Sohn: Plastic Deformation and Life Prediction of Solder Joints for Mechanical Shock and Drop/Impact Loading Conditions. ECTC 2007.

18. Yeh/ Lai/ Wang: Parametric Study on Board-Level Electronic Test Device Subjected to JEDEC Vibration Loads. International Conference on Electronic Packaging Technology & High Density Packaging (ICEPT-HDP) 2008.

19. Yeh/ Lai: Strain-rate and Impact Velocity Effects on Joint Adhesion Strength. ICEPT-HDP 2008.

20. Pang/ Che: Drop Impact Analysis of Sn-Ag-Cu Solder Joints Using Dynamic High-Strain Rate Plastic Strain as the Impact Damage Driving Force. ECTC 2006.

21. Lall/ Grupte/ Choudhary: Cohesive-Zone Explicit Sub-Modeling for Shock Life-Prediction in Electronics. ECTC 2007.

22. Song/ Lee/ Clark: Characterization of Failure Modes and Analysis of Joint Strength Using Various Conditions for High Speed Solder Ball Shear and Cold Ball Pull Tests. ECTC 2007.

23. Syed/ Kim/ Lin: A Methodology for Drop Performance Prediciton and Application for Design Optimization of Chip Scale Packages. ECTC 2005.

24. Wen/ Fu/ Zhou: Dynamic Properties Testing of Solders and Modeling of Electronic Packages Subjected to Drop Impact. ICEPT-HDP 2008.

25. Yeh/ Lai/ Kao: Evaluation of Board-Level Reliability of Electronic Packages under Consecutive Drops. Microelectronics Reliability 46 (2006), p1172-1182.

26. Kim/ Noguchi/ Amagai: Vibration Fatigue Reliability of BGA-IC Package with Pb-Free solder and Pb-Sn Solder. Microelectronics Reliability 46 (2006), p459-466.

27. Song/ Lee/ Newman: Effect of Thermal Aging on High Speed Ball Shear and Pull Tests of SnAgCu Lead-free Solder Balls. ECTC 2007.

28. Lou/ Wen/ Chen: The Effect of Strain Rate and Strain Range on Bending Fatigue Test. ICEPT-HDP 2008.